Available online at www.sciencedirect.com
SCIENCE DIRECT®
Journal of Sound and Vibration 283 (2005) 707–722
JOURNAL OF SOUND AND VIBRATION
www.elsevier.com/locate/jsvi

Feasibility study of a tunable friction damper

Joon-Hyun Lee[a], Ed Berger[b], Jay H. Kim[b,*]

[a]*Applied Acoustics and Vibration Lab, Samsung Electronics, Suwon, Korea*
[b]*Structural Dynamics Research Lab, Mechanical, Industrial and Nuclear Engineering Department, University of Cincinnati, Cincinnati, OH 45221-0072, USA*

Received 11 December 2002; accepted 10 May 2004
Available online 23 November 2004

Abstract

A new design of friction damper is proposed and called the tunable friction damper. The design is proposed as an alternative to a conventional sliding mass-type friction damper, which is commonly used to reduce vibration in rotating systems. The design combines advantages of the friction damper, which dissipates energy via sliding friction, and the spring-mass-type vibration damper, which absorbs energy by its own vibration. The tunable damper is designed to work as a friction damper while the mass slips and as a vibration absorber while the mass sticks, during which the conventional friction damper ceases to function as a damper. The most important advantage of the design is that the damper can be tuned for a large reduction of the vibration in a narrow frequency range of choice while providing damping in a broad range of frequency as well. Despite its simple concept, design analysis of the system is difficult due to the nonlinear dynamics of the system. Numerical simulations are employed to demonstrate the feasibility of the concept, and to understand the roles of major design parameters. It is shown that proper sizing of the mass and the compliance of the damper allows the design to exploit benefits of both the friction damper and vibration absorber.

*Corresponding author. Tel.: +1-513-556-6300; fax: +1-513-556-6300.
E-mail address: jay.kim@uc.edu (J.H. Kim).

0022-460X/$ - see front matter © 2004 Elsevier Ltd. All rights reserved.
doi:10.1016/j.jsv.2004.05.022

1. Introduction

Increased use of high-strength materials and integral constructions in modern rotating machinery such as jet engines and turbines tends to reduce damping in the system, thus making the system susceptible to vibration-related failures. Various friction dampers have been used to provide dissipation in such systems, including the commonly adopted sliding mass-type design. One problem associated with the friction damper is the difficulty in quantitative design analysis due to the nonlinear nature of the related motion. Extensive study has been conducted in the past two decades to develop tools for design and analysis of friction dampers [1–5]. Approximate or numerical analysis is used in most works because of the nonlinear aspect of the problem. The harmonic balance method (HBM) is a semi-analytical approximate method to solve friction induced motion problems by many researchers [1–5]. Because of the complexity of the problem, all studies employ significant simplifications in modeling the system dynamics.

While qualitative studies can be conducted based on simple one or two degree-of-freedom (dof) models, more generalized models are necessary for quantitative analyses. Lumped parameter models can be generalized by assigning more dofs to the system model as done by many investigators [6,7]. Such models provide more information, for example partial slip conditions; however, choosing meaningful system parameters becomes increasingly difficult as dofs increase. Models described as a continuous system based on the FEM formulation found in some recent works [8] seem attractive. The approach is still limited to substantially approximated system models because of the required computational intensity. Another problem is that not only the analysis itself but also the interpretation of the results becomes increasingly difficult as the model becomes more complex.

This paper proposes a new *design* concept, the tunable friction damper, which combines a sliding mass type friction damper and a vibration absorber. First, the numerical integration program to be used in this work is validated by applying the program to a known, reported problem. The problem is solved by the HBM as well, and reported solutions obtained by the numerical integration and the HBM are compared to those obtained by the authors' procedure. Then, the new design is introduced, and its basic behavior and unique features are explained based on the results from numerical simulations. Parameter studies of the main design variables are also conducted.

2. Validation of the numerical integration

A single dof system with friction damper joint is shown in Fig. 1. Inertia, stiffness and damping elements M, K and C represent dynamics of the blade, while the stiffness K_d and the friction joint represent dynamics of the interface between the blade and the sliding mass. The model shown in Fig. 1 has been used in earlier works in this area by many investigators for fundamental study of dynamics of friction dampers [1–3]. Menq et al. [3] used the HBM to solve the problem when the normal force varies as a linear function of the displacement of the motion. The problem is solved again in this work both by the HBM and the numerical integration, and the results are compared with the reported results in Ref. [3] for validation purpose. After the validation, the numerical integration is used as the tool for design studies.

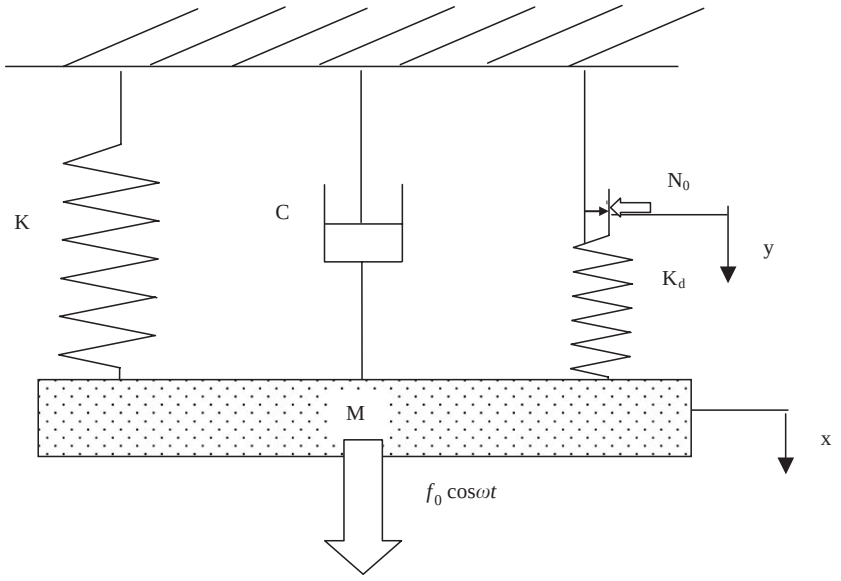

Fig. 1. Single-dof system with friction damper.

2.1. Equation of motion

The equation of motion of the system shown in Fig. 1 is

$$M\ddot{x}(t) + C\dot{x}(t) + Kx(t) = f_0 \cos \omega t - f_n(t), \tag{1}$$

where $f_n(t)$ is the nonlinear force acting at the friction joint. The joint will slide when the magnitude of f_n becomes equal to μN. The contact force N is considered a linear function of the displacement as

$$N(x) = N_0 + \gamma K_d x(t) \quad \text{if } x \geqslant -N_0/(\gamma K_d). \tag{2}$$

The contact force is constrained to be larger than zero by imposing the condition that $x < -N_0/(\gamma K_d)$. N_0 is the nominal contact force and γ represents the coupling ratio between the motion and force [3]. It is noted that the normal contact force is generated by the centripetal force, and therefore is proportional to the mass.

2.2. Representation of nonlinear force

As can be seen in Fig. 1, the nonlinear friction force is $f_n = K_d(x - y)$, which is at the same time constrained to be no larger than the sliding friction force $\pm\mu N$. The friction force f_n is shown in Fig. 2 when the normal force is coupled with the motion as in equation (2). Fig. 3 is a special case of Fig. 2 when the coupling factor γ=0.

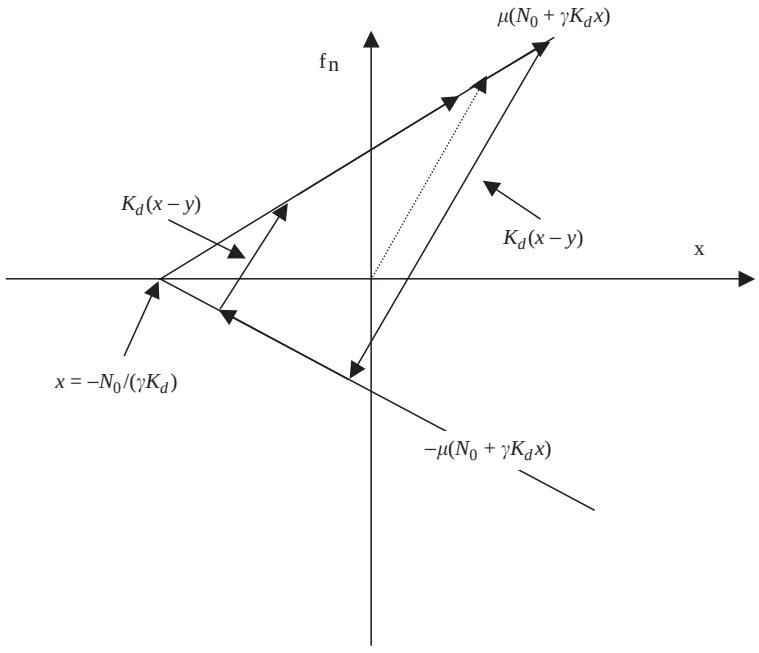

Fig. 2. A piecewise–linear–nonlinear force with coupling effect.

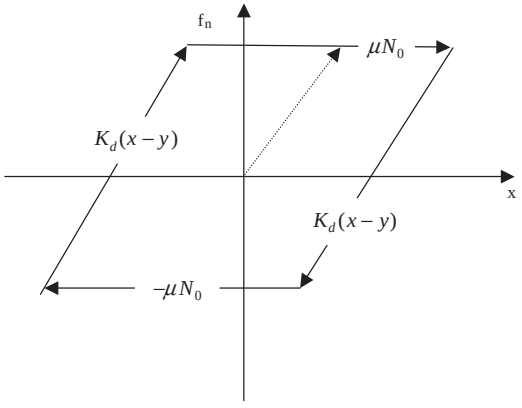

Fig. 3. A piecewise–linear–nonlinear force without coupling effect.

2.3. HBM solution

The HBM is an approximate method for solving friction-induced vibration problems [2]. While a multi-term solution is possible, our case is limited to the one-term solution used in Refs. [1–3]

because the problem is solved for validation purposes. The procedure can be summarized as follows:

(1) Approximate the motion as harmonic with assumed displacement amplitude and phase.
(2) Construct the nonlinear force–displacement diagram based on the assumed motion and friction conditions (stick-slip conditions).
(3) Convert the force–displacement diagram to the force–angular displacement, i.e. force–time diagram. Approximate this force as a one-term Fourier series.
(4) Using this one-term approximation of the nonlinear force, solve the equation of motion of the system to obtain the displacement and the phase.
(5) Check if the assumed displacement amplitude is correct. If not, repeat the procedure with new assumed displacement amplitude. The procedure is repeated until the solution converges.

Now a system defined by $f_0 = 1$, $K = 0.9$, $c = 0.01$, $M = 1.0$ and $K_d = 0.1$ is considered, which was the system solved in Ref. [3]. The displacement is represented as

$$x(t) = A\cos(\omega t - \psi) + B = A\cos\theta + B, \tag{3}$$

where $\theta = \omega t$, ψ is the phase delay of the response and B is the offset, which becomes zero if the coupling factor is zero (the case of Fig. 3). The amplitude A and offset B obtained as functions of the excitation frequency are shown in Figs. 4 and 5. Note that Fig. 4 is actually the frequency response function (FRF) because f_0=1 is used. Fig. 4 shows the result when the coupling is weak ($\mu\gamma = 0.1$) and Fig. 5 shows when it is strong ($\mu\gamma = 0.6$). Calculations were made for the frequency

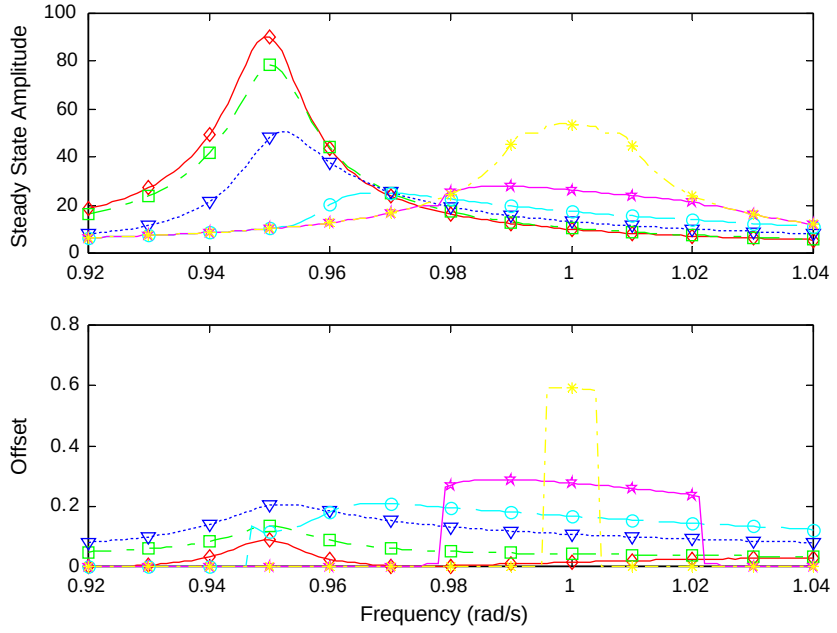

Fig. 4. System response obtained by HBM when dynamic coupling is weak: $\mu\gamma = 0.1$, $K = 0.9$, $C = 0.01$, $M = 1.0$, $K_d = 0.1$, and $\mu N_0 = -0.2$ (—◇—), 0.1 (···□···), 0.5 (---▽---), 1 (-·○·-), 2 (—☆—), 5 (-·×·-).

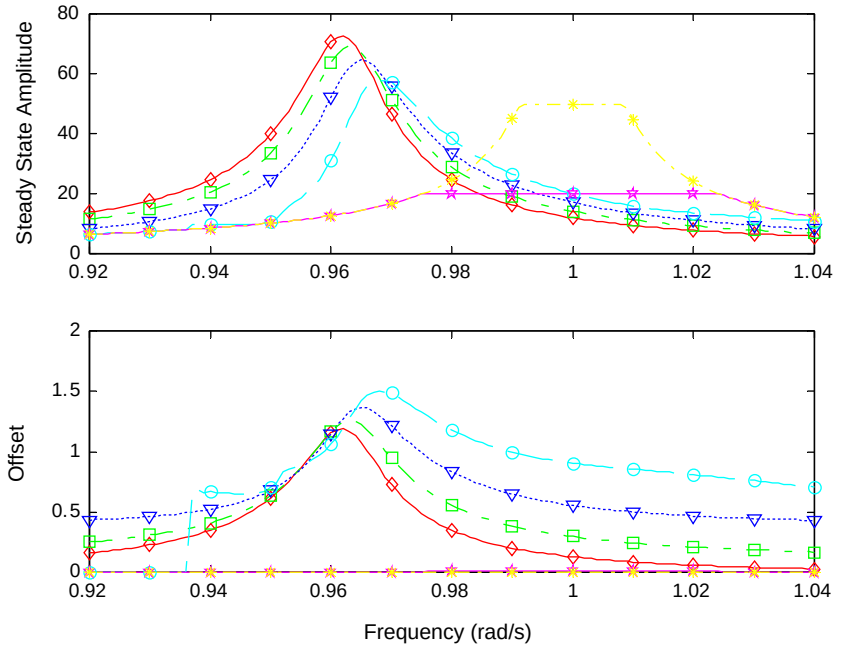

Fig. 5. System response obtained by HBM when dynamic coupling is strong: $\mu\gamma = 0.6$, $K = 0.9$, $C = 0.01$, $M = 1.0$, $K_d = 0.1$, $f_0 = 1$, and $\mu N_0 = -0.2$ (—◇—), 0.1 (···□···), 0.5 (---▽---), 1 (-·-○-·-), 2 (—☆—), 5 (···×···).

range between 0.92 and 1.04 at the frequency interval of 0.01 for six levels of the static preloads, $N_0 = -0.2$, 0.1, 0.5, 1, 2, 5. Note that the $N_0 = -0.2$ case yields zero normal force, therefore corresponds to the system without the friction damper.

The results shown in Figs. 4 and 5 are identical to those reported in Ref. [3]. As shown in the figures, the peak amplitude depends on the magnitude of the normal force. Initially, the peak decreases as the normal force increases until the friction limit μN_0 reaches 1.0. Then the peak starts to increase as μN_0 increases beyond 2.0. This indicates that there will be an optimum normal force to ensure the maximum damping effect [1–3]. A too large normal force will make the friction damper stick most of the time, thereby decreasing the total energy dissipation. At a very high normal force, say $\mu N_0 = 5$, the mass always sticks, and provides no energy dissipation, which is also confirmed from the fact that the resonance peaks in Figs. 4 and 5 move to $\omega = \sqrt{(K_d + K)/M}$ when $\mu N_0 = 5$.

2.4. Solutions by numerical integration

A direct numerical integration method is utilized for the analysis of the proposed tunable friction damper. The specific analysis method will have to be chosen based on the accuracy requirement and computational resources. A numerical integration procedure is applied to the problem discussed in Section 2.3 for validation purpose. Numerical integration of Eq. (1), with the force–displacement relationship defined in Eq. (2) as the constraint, is conducted using the SIMULINK toolbox in MATLAB [9]. The integration starts from a set of assumed initial

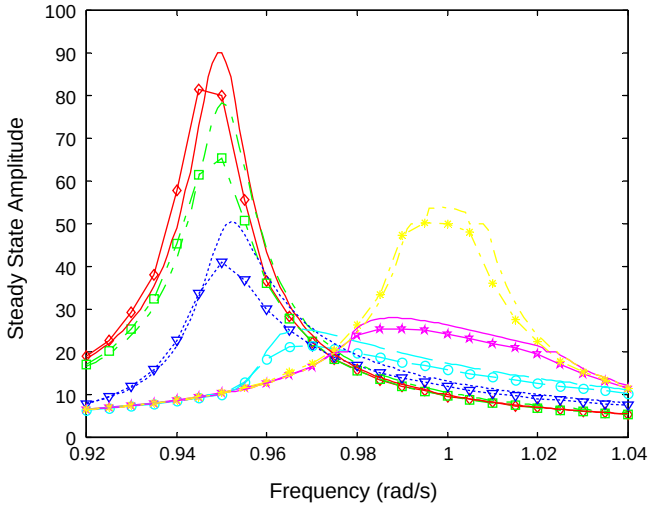

Fig. 6. Comparison of responses calculated from HBM and numerical integration; lines with center symbols are numerical integrations; lines without symbol are HBM solutions. The cases shown are for $\mu\gamma = 0.01$ (weak coupling), $K = 0.9$, $C = 0.01$, $M = 1.0$, $K_d = 0.1$, $f_0 = 1$, and $\mu N_0 = -0.2$ (—◇—), 0.1 (- -□- -), 0.5 (---▽--), 1 (- -○- -), 2 (—☆—), 5 (- -×- -).

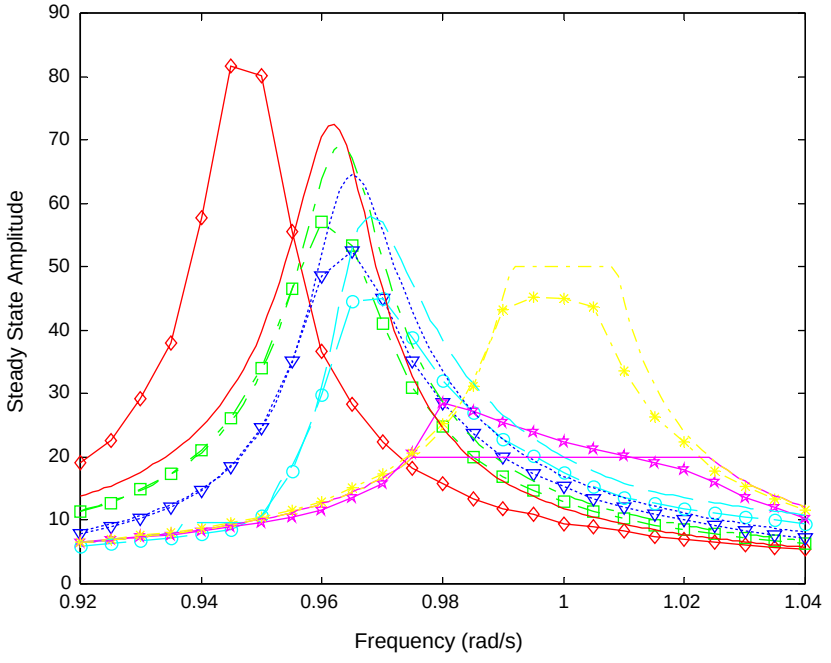

Fig. 7. Comparison of responses calculated from HBM and numerical integration; lines with center symbols are numerical integrations; lines without symbol are HBM solutions. The cases shown are for $\mu\gamma = 0.6$ (strong coupling), $K = 0.9$, $C = 0.01$, $M = 1.0$, $K_d = 0.1$, $f_0 = 1$, and $\mu N_0 = -0.2$ (—◇—), 0.1 (- -□- -), 0.5 (---▽--), 1 (- -○- -), 2 (—☆—), 5 (- -×- -).

conditions and continues until a converged result is achieved. In these examples, converged results were typically obtained after 150–200 cycles of integration.

Figs. 6 and 7 compare the results from the HBM with the results from numerical integrations. Because the HBM solution is approximate, the two sets of results are similar but not exactly the same. As expected, the difference in solutions becomes larger as the nonlinear effect increases, i.e. the damping effect becomes larger also as the coupling effect becomes larger. The numerical integration results are well correlated with the HBM solutions and explain the system behavior as expected.

3. Tunable friction damper

3.1. Basic idea

Now a new design concept, a tunable damper, is considered. The idea is to combine the advantages of a passive vibration absorber and a friction damper. Fig. 8 illustrates the damper design, which shows two masses connected by a spring. In actual design, a relatively compliant material of smaller cross-sectional area than the mass can be used as the spring. While a friction damper should be designed very stiff in the direction of the normal force to endure the large centrifugal force, the flexibility of the proposed tunable damper is acting in the direction in which no large forces are acting.

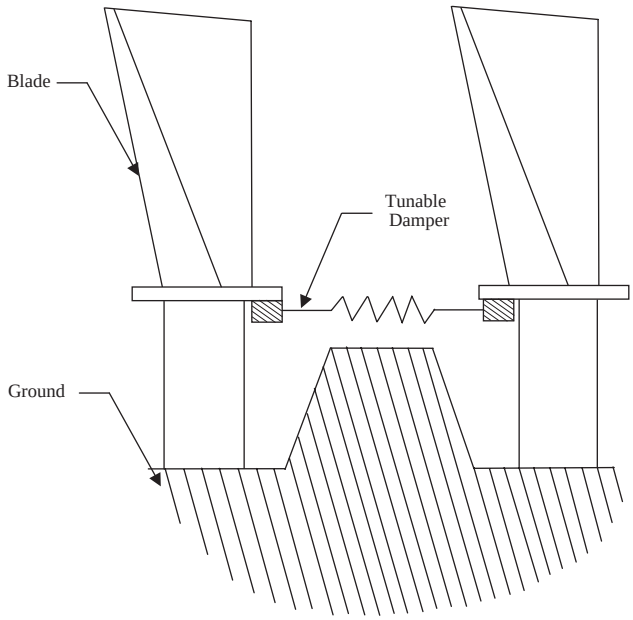

Fig. 8. Proposed design of tunable damper.

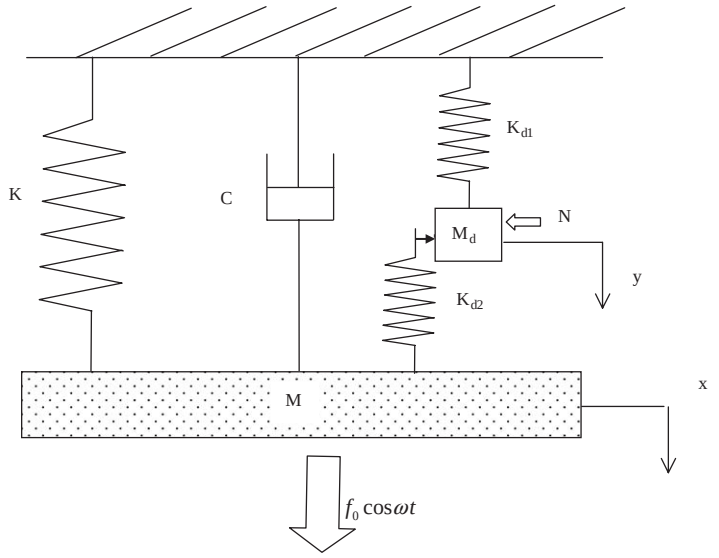

Fig. 9. Single-dof system model of the tunable damper.

Because the blade system shown in Fig. 8 is not geometrically symmetric, its vibration modes will be in general composed of both symmetric and antisymmetric components. The friction dampers, tunable as well as rigid, are effective only on symmetric components of the motion, in which the two blades move to opposite directions. Therefore, the model can be reduced to the system shown in Fig. 9. In this figure, M_d represents the mass of the damper, K_{d1} represents the stiffness of the connecting spring shown in Fig. 8, K_{d2} represents the effective stiffness of the blade and damper interface, and M and K represent the effective inertia and stiffness of the blade at the frequency of motion in consideration.

During the stick motion (when the damper mass is not sliding), the friction damper will behave as a vibration absorber whose tuning frequency is

$$\omega_d^2 = (K_{d1} + K_{d2})/M_d. \tag{4}$$

Therefore, ω_d is the tuning frequency at which the damper absorbs most of the vibration energy of the system.

3.2. Analysis of the system

The motion of the system depicted in Fig. 9 is described by the following two equations:

$$M\ddot{x}(t) + C\dot{x}(t) + Kx(t) = f_0 \cos \omega t - f_n(t), \tag{5}$$

$$M_d\ddot{y} + K_{d1}y = f_n(t). \tag{6}$$

Again, f_n is the nonlinear friction force, which is depicted in Fig. 2.

In the system of this case study, system parameters are chosen as $M=1$, $C=0.1$, $K=0.9$, $K_d=0.1$; therefore, the natural frequency of the blade $\omega_b \approx 0.949$. Note that the two springs behave as a single spring of rate $K_d=K_{d1}+K_{d2}$ when the sliding mass sticks. The tuner mass M_d is determined from Eq. (4) to make the damper tuning frequency $\omega_d = \omega_b$.

3.3. Basic system response characteristics

Fig. 10 shows a typical result of the time integration for the blade and the tuner mass responses in the time domain. Converged responses are attained typically after 150–200 cycles of the calculated motion.

3.3.1. System responses at the tuning frequency

Fig. 11 shows the effect of the tunable damper when the damper frequency is tuned to the natural frequency of the blade ($\omega_d = \omega_b$). A very light dynamic coupling case is considered ($\mu\gamma = 0.01$). Four different levels of the normal force have been applied, which result in friction forces of $\mu N_0 = -0.2$, 1, 2, 5, 10. The first case is actually when the normal force is zero, and the friction damper is inactive.

Effects of both the friction damper and the vibration absorber can be seen in the figure. The absorber effect is seen from the significant reduction of the response in the narrow frequency range around the tuning frequency. Two response peaks arise away from the tuning frequency, which is expected because the system becomes a 2 dof system when the damper is active. As the normal force increases beyond a threshold value, the performance of the damper as the friction

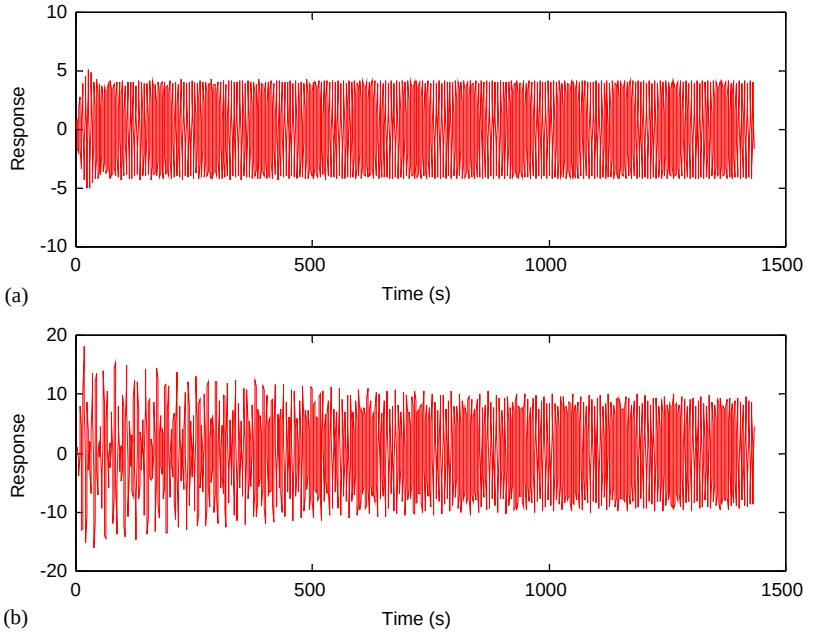

Fig. 10. Displacement responses of the main and tuner masses calculated by numerical integration: (a) blade, (b) tuner.

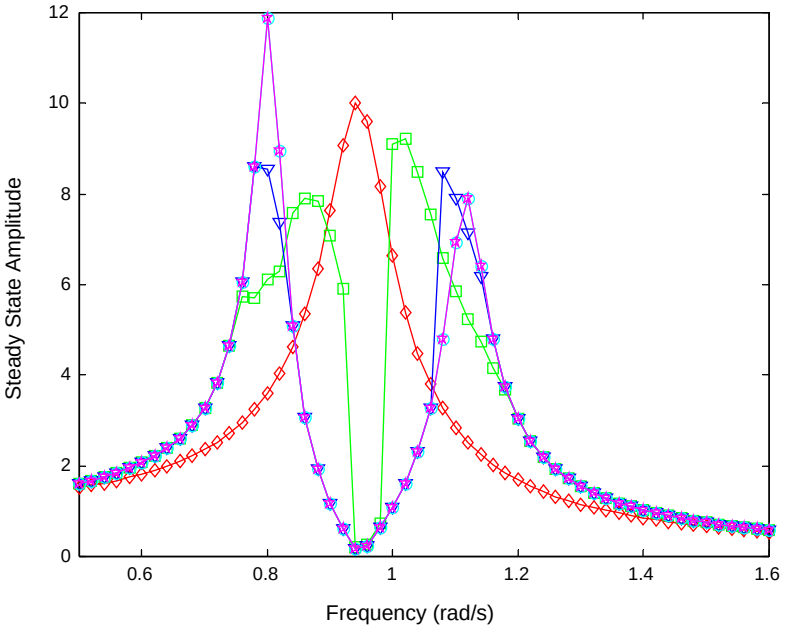

Fig. 11. Frequency resonse of the tunable damper when $\omega_d = \omega_b$, $\mu\gamma$=0.01, K=0.9, C=0.1, M=1.0, K_d=0.1, M_d=0.111, when $\mu N_0 = -0.2$ (—◇—), 0.1 (-·□·-), 0.5 (---▽---), 1 (-·○·-), 2 (—☆—), 5 (-·×·-).

damper diminishes because the mass sticks most of the time. In this example, the results when $\mu N_0 = 5$ and 10 are almost identical, which indicates that the sliding motion does not occur in these cases, i.e. the mass sticks all the time. The damper in this case acts as a pure vibration absorber without the friction effect. At μN_0=1 and 2, the two peak responses become lower than those of the $\mu N_0 = 5$ and 10 cases, which indicates that energy is dissipated by the sliding motion, the virtue of the friction damper. The two peaks that correspond to the μN_0=1 and 2 cases are lower than the single peak that corresponds to $\mu N_0 = 0$ case, the no damper case. The μN_0=2 case shows the best result among the test cases. Therefore, in practice, an optimal magnitude of the normal force, i.e. mass, will have to be determined first as in conventional friction dampers [1], then the tuner stiffness K_{d2} can be determined correspondingly to obtain the desired tuning frequency.

Comparing the effect of the tunable damper shown in Fig. 11 with those of the rigid friction damper shown in Figs. 4 and 5, it becomes obvious that the tunable damper does not always provide better performance. The new damper is very effective to reduce vibration amplitudes in the vicinity of the design frequency, which is much like the traditional vibration absorber or a band filter in general. Thus, the tunable damper will have to be designed by matching the design frequency with the dominant operating excitation frequencies.

3.3.2. *System responses at various tuning frequencies*

Now we consider three cases, which are when the tuner frequency is much higher than, almost equal to, and much lower than the blade frequency. Keeping in mind that $K_d = K_{d1} + K_{d2}$:

Case 1: $\omega_d \gg \omega_b$

$$\omega_d = \sqrt{\frac{K_d}{M_d}} = \sqrt{\frac{0.1}{0.05}} = 1.414 \approx 1.5\omega_b.$$

Case 2: $\omega_d = \omega_b$

$$\omega_d = \sqrt{\frac{K_d}{M_d}} = \sqrt{\frac{0.1}{0.111}} = 0.949 \approx \omega_b.$$

Case 3: $\omega_d \ll \omega_b$

$$\omega_d = \sqrt{\frac{K_d}{M_d}} = \sqrt{\frac{0.1}{0.3}} = 0.577 \approx 0.6\omega_b.$$

To vary the tuner frequencies, the tuner mass was varied to $M_d = 0.05/0.111/0.3$ while keeping K_d the same.

Figs. 12(a) and (b) show the responses of the blade and tuner for those three cases when $\mu N_0 = 1$. As seen in Fig. 12(a) a noticeable effect on the system response occurs only in the vicinity of the tuning frequencies in all three cases. Comparing Figs. 12(a) and (b), the tuner mass moves with much higher amplitude than the blade mass, especially around the tuning frequency, which is a typical behavior of the vibration absorber. Figs. 13–15 show the system responses for the same three tuning frequencies.

3.4. Study of design parameters

Based on this numerical study, the tunable damper should be designed by determining the tuning frequency in relation to the resonance frequencies and operating speed of the system. For

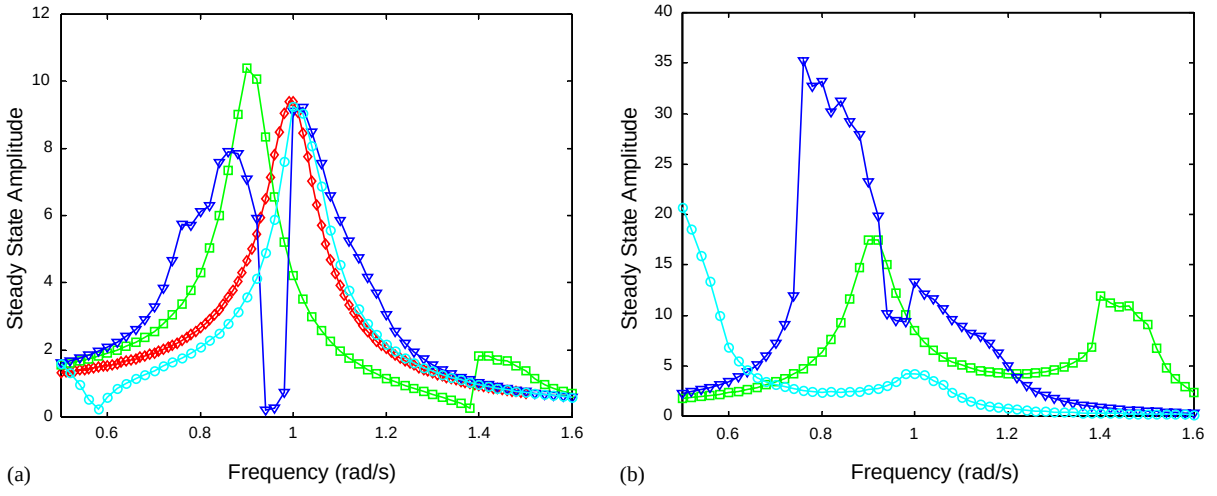

Fig. 12. Frequency response of (a) the main mass and (b) of the tuner mass of the tunable damper: $\mu N_0 = 1.0$, $\mu\gamma = 0.01$, $K = 0.9$, $C = 0.01$, $M = 1.0$, $K_d = 0.1$; $M_d = 0.05(\omega_d > \omega_b)$: —□—; $M_d = 0.111(\omega_d = \omega_b)$: —▽—; $M_d = 0.3(\omega_d < \omega_b)$: —○—; 1 dof response in (a): —◇—.

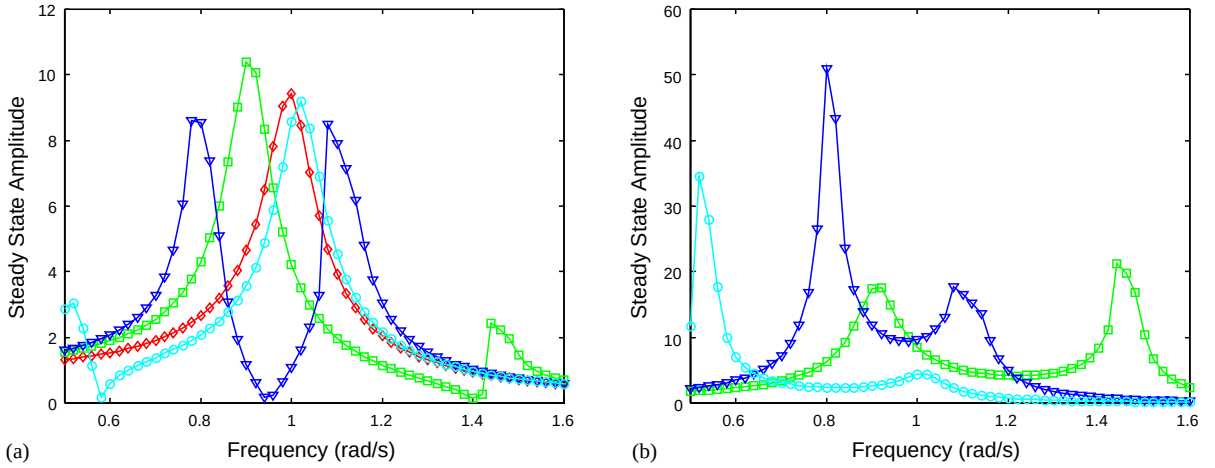

Fig. 13. Frequency response of (a) the main mass and (b) the tuner mass of the tunable frictional damper: $\mu N_0 = 2.0$, $\mu\gamma = 0.01$, $K = 0.9$, $C = 0.1$, $M = 1.0$, $K_d = 0.1$, $M_d = 0.05(\omega_d > \omega_b)$: —□—; $M_d = 0.111$ $(\omega_d = \omega_b)$: —▽—; $M_d = 0.3(\omega_d < \omega_b)$: —○—; 1 dof response in (a): —◇—.

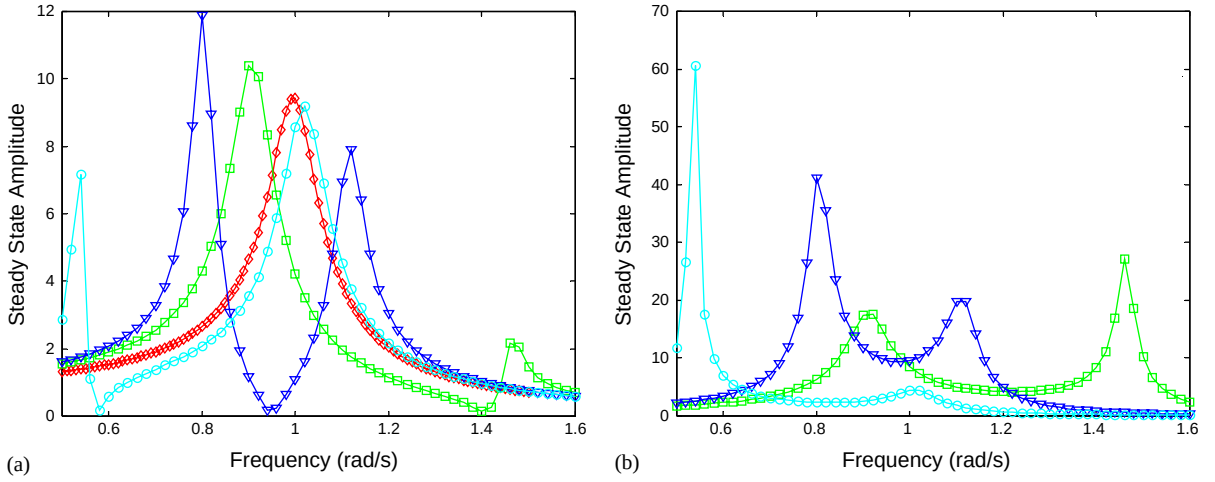

Fig. 14. Frequency response of (a) the main mass and (b) the tuner mass of the tunable damper: $\mu N_0 = 5.0$, $\mu\gamma = 0.01$, $K = 0.9$, $C = 0.1$, $M = 1.0$, $K_d = 0.1$, $M_d = 0.05(\omega_d > \omega_b)$: —□—, $M_d = 0.111$ $(\omega_d = \omega_b)$: —▽—; $M_d = 0.3(\omega_d < \omega_b)$: —○—; 1 dof response in (a): —◇—.

example, the tuning frequency may be matched to a critical speed that is closest to the steady-state operating speed. At the designed frequency, the damper effectively works as a vibration damper, taking away the vibration energy of the main system, thus reducing the system response significantly. The two new resonance peaks could be a potential problem, which is an issue that must be addressed in the design process of the vibration absorber. The problem can be alleviated by the effect of the friction damper lowering the two peaks. In any case, the designer has at his/her

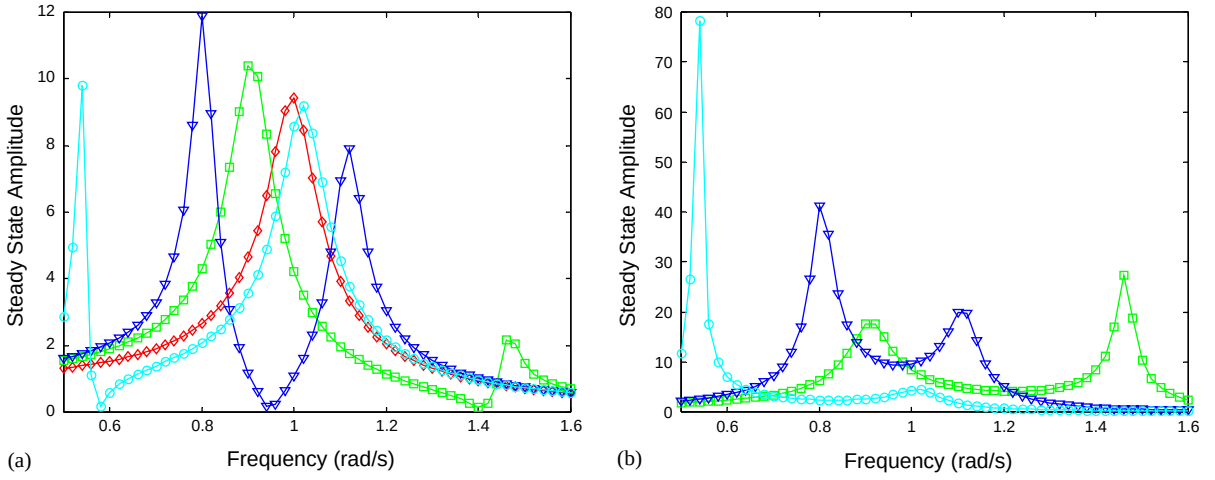

Fig. 15. Frequency response of (a) the main mass and (b) the tuner mass of the tunable damper: $\mu N_0 = 10.0$, $\mu\gamma = 0.01$, $K = 0.9$, $C = 0.01$, $M = 1.0$, $K_d = 0.1$, $M_d = 0.05(\omega_d > \omega_b)$: —□—; $M_d = 0.111$ $(\omega_d = \omega_b)$: —▽—; $M_d = 0.3(\omega_d < \omega_b)$: —○—; 1 dof response: —◇—.

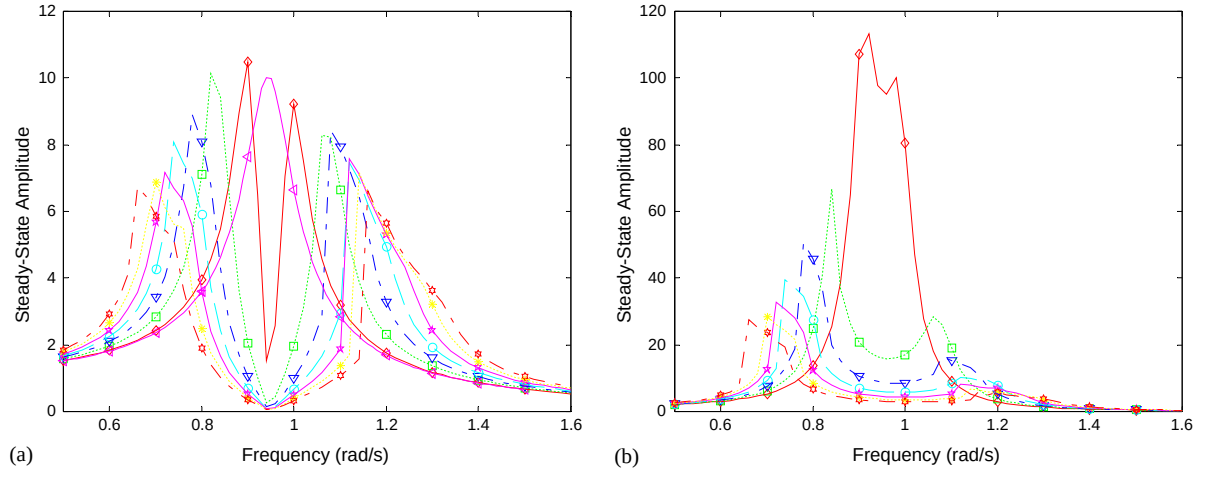

Fig. 16. Sensitivity of the response of (a) the main mass and (b) the tuner mass of the tunable frictional damper to the stiffness of the tuner, $\mu N_0 = 2.0$, $\mu\gamma = 0.01$, $K = 0.9$, $C = 0.01$, $M = 1.0$. Stiffness variations: —◇—, 1%; ·□·, 6%; --▽--, 11%; --○--, 16%; —☆—, 21%; ·×·, 26%; —✡—, 31%; —◁—, 1 dof.

discretion one more design parameter, tuning frequency, than using the conventional sliding mass damper.

The stiffness, K_d (or mass, M_d) of each tuner design is varied within 1–40% of the stiffness, K (or mass, M) of the main mass by 5% at a time. By varying the tuner stiffness, the optimum design value for the tunable frictional damper system could be observed. It has to be noted that the tuning frequency is fixed at the system resonance frequency; therefore, the mass also increases as

much as the stiffness increases. Therefore, a larger stiffness implies a physically larger friction damper. Fig. 16 shows the response of the main mass and the tuner for various tuner designs at the condition of $\mu N_0 = 2.0$, $K = 0.9$, $C = 0.01$, $M = 1.0$. From the figure, it is seen that the effect of the damper becomes larger as the stiffness and mass (or the size) of the tuner increase, as expected.

In practice, the tunable friction damper provides one additional design parameter, the tuning frequency, to designers. From the designer's standpoint, it is an advantage that the tuner stiffness (K_{d1}) is a clearly defined parameter that can be applied easily. For example, the stiffness of the blade–damper interface K_{d2}, the only stiffness parameter in the conventional friction damper, is not only difficult to estimate (it is obtained by approximating the dynamics of the blade to an equivalent, simple model) but also not free to change for the purpose of designing the damper (K_{d2} is given by the blade design, not by the need for the damper design).

4. Conclusions

A new concept of friction damper design is proposed in this work. The key idea is combining the features of a vibration absorber and a sliding friction damper into one design. The damper is designed to work as a vibration absorber during the time while the sliding mass sticks to the blade base, therefore ceases to work as a friction damper, and works as a friction damper when the mass is sliding. Hence, the damper possesses both characteristics of the passive vibration absorber and the sliding friction damper. Properly designed, the damper can provide good energy dissipation as well as a sharp reduction of the response amplitude in the narrow frequency range of design. As the damper partially works as a friction damper, a proper level of the friction force has to be provided by adjusting the mass for best performance. As typical vibration absorbers do, the new design induces two resonance peaks away from the design frequency, which may cause problems in some cases. These peaks may be reduced substantially by the effect of the friction damper aspect of the system. Design principles of vibration absorber may be applied; however, they will have to be checked by numerical simulations because the nonlinear effect may cause unexpected result.

The new tunable damper concept provides designers one design parameter they can easily control, namely the tuning frequency, which can be used to shift the resonance peaks while retaining some of the broadband amplitude reduction effect of the friction damper. Another potentially significant advantage of the new design is the ease of implementing the design because the key design variable, the stiffness of the friction damper, is well defined and easy-to-change.

References

[1] J.H. Griffin, Friction damping of resonant stresses in gas turbine engine airfoils, *Journal of Engineering for Power* 102 (1980) 329–333.

[2] C. Pierre, A.A. Ferri, E.H. Dowell, Multi-harmonic analysis of dry friction damped systems using an incremental harmonic balance method, *Journal of Applied Mechanics* 52 (1985) 958–964.

[3] C.H. Menq, J.H. Griffin, J. Bielak, The influence of a variable normal load on the forced vibration of a frictionally damped structure, *Journal of Engineering for Gas Turbines and Power* 108 (1986) 300–305.

[4] K.Y. Sanliturk, D.J. Ewins, Modeling two-dimensional friction contact and its application using harmonic balance method, *Journal of Sound and Vibration* 193 (2) (1996) 511–523.
[5] J.H. Wang, W.K. Chen, Investigation of the vibration of a blade with friction damper by HBM, *Journal of Engineering for Gas Turbines and Power* 115 (1993) 294–299.
[6] C.H. Menq, J. Bielak, J.H. Griffin, The influence of microslip on vibratory response—part I: new microslip model, *Journal of Sound and Vibration* 107 (2) (1986) 279–293.
[7] E.J. Berger, C.M. Krousgrill, On friction damping modeling using bilinear hysteresis elements, *Journal of Vibration and Acoustics* 124 (3) (2002) 367–375.
[8] E.J. Berger, M.R. Begley, M. Mahajani, Structural dynamic effects on interface response-formulation and simulation under partial slipping conditions, *Journal of Applied Mechanics* 67 (2000) 785–792.
[9] MATLAB SIMULINK Manual 2001, Version 2, The Math Works, Inc.